2006
VOLUME 1
NUMBER 3

Material Matters™

Chemistry Driving Performance

ALDRICH®

Deposition of Ceramic and Hybrid Materials

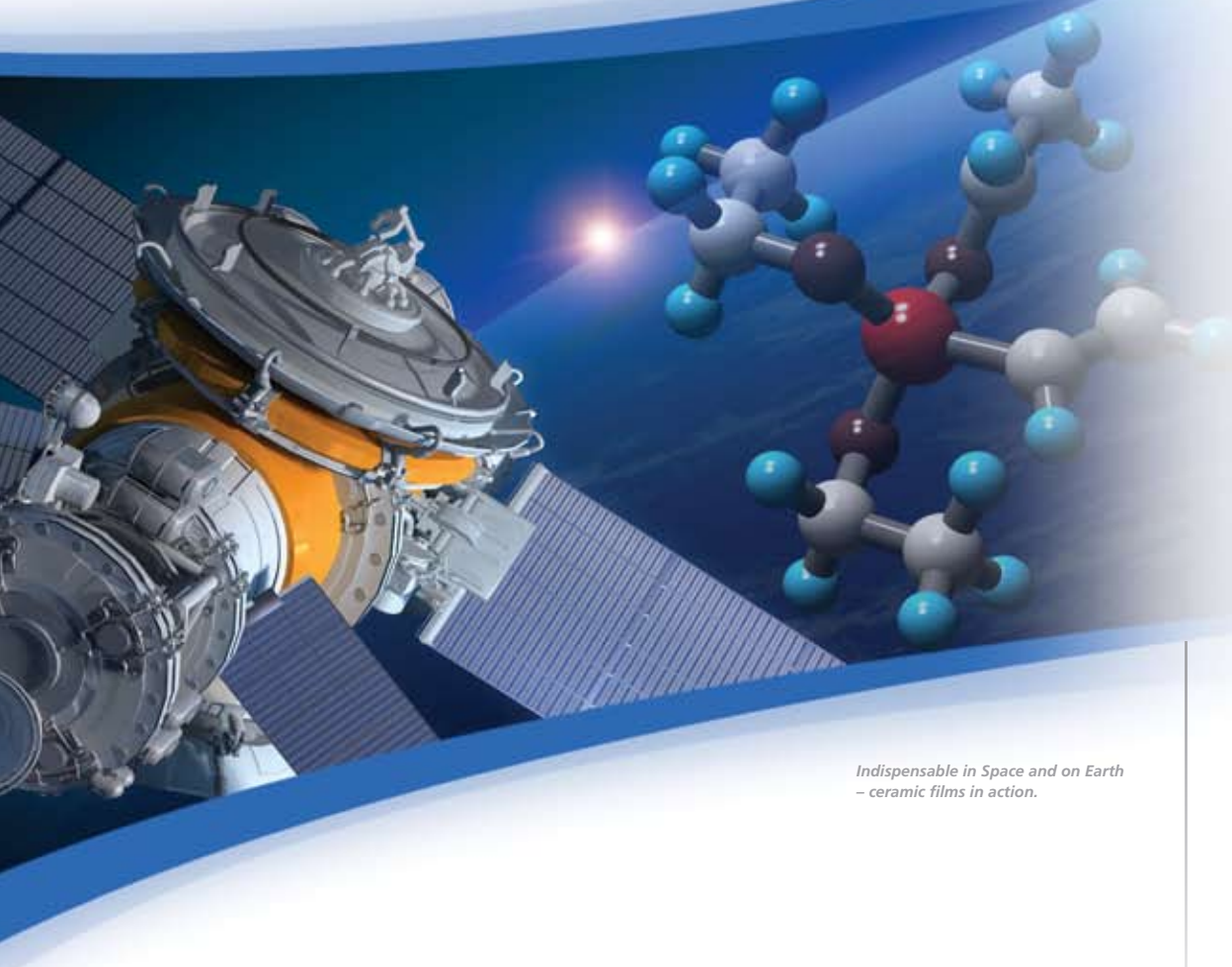

Indispensable in Space and on Earth – ceramic films in action.

Chemical Deposition Techniques in Materials Design

Savannah ALD System

Sol-Gel Science for Ceramic Materials

Hermetic Barrier Using Vinyl Triethoxysilane (VTEOS)

Silicon-Based Passive and System-in-Package Integration

Vacuum Deposited Non-Precious Metal Catalysts for PEM Fuel Cells

sigma-aldrich.com

SIGMA-ALDRICH

Introduction

Welcome to the third issue of *Material Matters*™. This issue focuses on chemical deposition techniques and their application in electronics and alternative energy.

An introduction and comparison of chemical vapor deposition and solution deposition approaches to film fabrication is given by Dr. Balema of Sigma-Aldrich™ Materials Science. Scientists from Cambridge NanoTech discuss Chemical Vapor Deposition (CVD) and Atomic Layer Deposition (ALD), as well as advantages of the Savannah ALD system. Dr. Young from the US Army Research Laboratory highlights basics of sol-gel science for ceramic materials. The group of Prof. Klein from Rutgers University presents a paper on the development of a hermetic barrier using vinyl triethoxysilane (VTEOS) via Sol-Gel Processing. Dr. Roozeboom from Philips and Prof. Kessels from the University of Technology, Eindhoven, Netherlands, discuss the suitability of atomic layer deposition in the fabrication of Si-based integrated passives and System-in-Package integration. Finally, researchers from the 3M Company led by Dr. Atanasoski and Dr. O'Neill report on the use of vacuum deposition in the preparation of electrode materials for fuel cells. Products that accelerate your research in the fundamental and applied science of chemical deposition are highlighted. We invite your comments, questions and suggestions about *Material Matters*™ and materials of interest to you: **matsci@sial.com**.

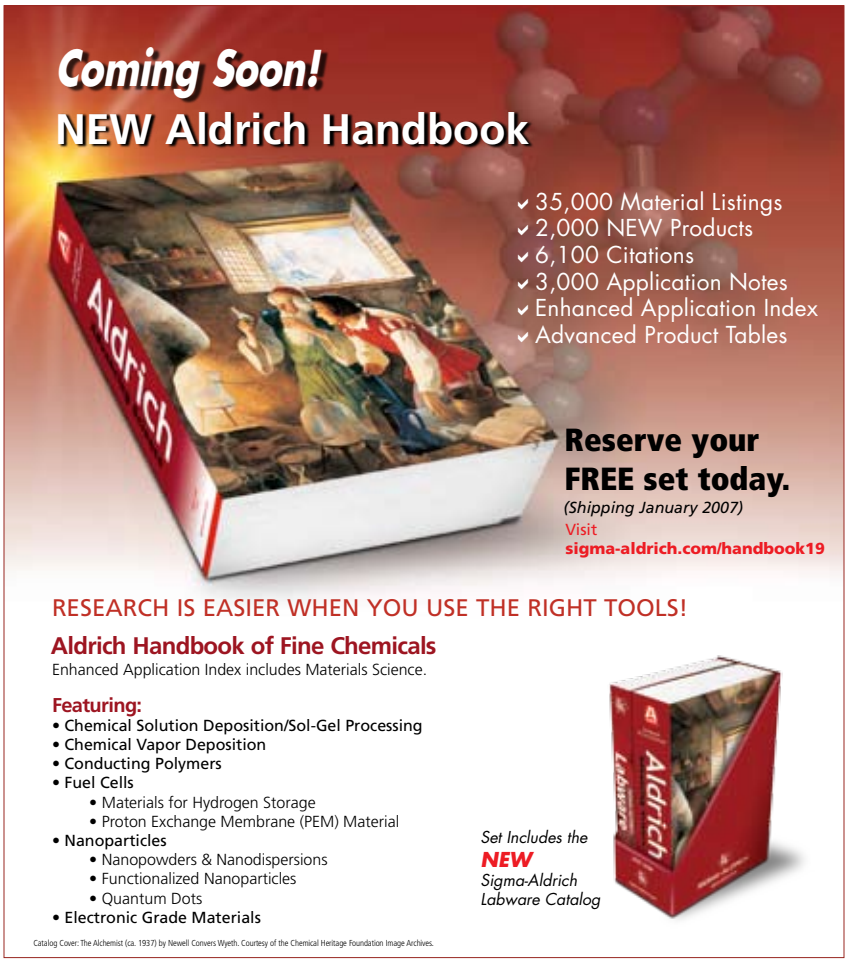

About Our Cover

The need for films and coatings is ubiquitous in the technological age we live. For example, films serving as humidity barriers form an essential part of microelectronics, micro-electromechanical systems and energy conversion devices. The cover depicts a molecule of vinyl triethoxysilane (VTEOS) that could be used to make a barrier film by chemical deposition. VTEOS is a multifunctional molecule that enables the generation of a hybrid silicon oxide film with polymerizable vinyl groups; the inorganic content is designed to be the barrier, while the hydrophobic, organic content repels water and fills porosity; for more details, please refer to the article by the Rutgers research group on page 11. As alluded to on the cover, such a film could be used to seal the elements of solar panels on a geosynchronous satellite for protection from the external environment.

Material Matters™
Chemistry Driving Performance

Vol. 1 No. 3

Aldrich Chemical Co., Inc.
Sigma-Aldrich Corporation
6000 N. Teutonia Ave.
Milwaukee, WI 53209, USA

To Place Orders

Telephone	800-325-3010 (USA)
FAX	800-325-5052 (USA)

Customer & Technical Services

Customer Inquiries	800-325-3010
Technical Service	800-231-8327
SAFC™	800-244-1173
Custom Synthesis	800-244-1173
Flavors & Fragrances	800-227-4563
International	414-438-3850
24-Hour Emergency	414-438-3850
Web Site	sigma-aldrich.com
Email	aldrich@sial.com

Subscriptions

To request your **FREE** subscription to *Material Matters*, please contact us by:

Phone: **800-325-3010** (USA)

Mail: **Attn: Marketing Communications**
Aldrich Chemical Co., Inc.
Sigma-Aldrich Corporation
P.O. Box 355
Milwaukee, WI 53201-9358

Email: **sams-usa@sial.com**

International customers, please contact your local Sigma-Aldrich office. For worldwide contact information, please see back cover.

Material Matters is also available in PDF format on the Internet at **sigma-aldrich.com/matsci**.

Aldrich brand products are sold through Sigma-Aldrich, Inc. Sigma-Aldrich, Inc. warrants that its products conform to the information contained in this and other Sigma-Aldrich publications. Purchaser must determine the suitability of the product for its particular use. See reverse side of invoice or packing slip for additional terms and conditions of sale.

All prices are subject to change without notice.

Material Matters is a publication of Aldrich Chemical Co., Inc. Aldrich is a member of the Sigma-Aldrich Group.

© 2006 Sigma-Aldrich Co.

Chemical Deposition Techniques in Materials Design

Dr. Viktor P. Balema
Sigma-Aldrich Materials Science

During the last decade, chemical deposition techniques have played an exceptionally important role in the design and manufacture of novel advanced devices. Physical deposition techniques, such as molecular beam epitaxy (MBE), physical vapor deposition (PVD) or sputtering, have been used for these applications. However, they suffer from limitations such as poor conformality, low throughput, restricted directional variation, and reduced compositional control. All of these issues can and have been addressed using chemical deposition techniques which offer additional advantages such as ultra-thin film growth. This is especially the case when layered inorganic materials are assembled in order to create an electronic chip or to modify the surface of a tool for improved performance and durability. Currently, two groups of different, yet related, techniques dominate the field. The first group comprising Chemical Vapor Deposition (CVD) and Atomic Layer Deposition (ALD) uses a gas phase to transport volatile molecules to the surface serving as a substrate. The second group of deposition techniques, called Chemical Solution Deposition or Sol-Gel Processing, uses a liquid phase as the mass transfer media.

There is a fundamental resemblance between these two groups - the way that the final material is created. In both cases, molecules of chemical compounds serving as precursors are delivered to the substrate surface and chemically modified to obtain the desired film. It should be noted, however, that the chemical transformations of the precursor in the case of CVD/ALD can occur in the gas phase and at the gas-solid interface, while in sol-gel processing it is carried out in solution (**Figure 1**). In the CVD/ALD approach, the chemical modification of the precursor is usually achieved via thermal conversion of precursor molecules and/or their reactions with molecules of other volatile precursors, or reactive gases such as oxygen or hydrogen.[1-3] Sol-gel processing consists of a sequence of chemical transformations in solution and solid-state. They include formation of a colloidal suspension in an appropriate solvent (sol), gelation (gel), evaporation of the solvent (drying), and thermal treatment (sintering). [4-7]

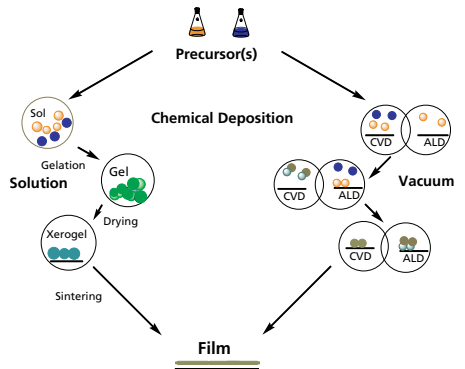

Figure 1. Schematic illustrating chemical deposition of ceramic films.

Materials with a layer thickness below 1 µm are called thin films, while thicker layers, especially those exceeding dimensions of a transistor in an electronic chip, are defined as thick films. Both thin and thick films play an exceptionally important role as elements of electronic and optical devices, computer memory chips, and in other related applications. Additionally, in the case of ceramic films, properties such as chemical resistivity and hardness enable their use as coatings on substrate materials and cutting tools for protection against corrosion, oxidation, and wear.

Typically, CVD/ALD techniques are methods of choice for the deposition of thin films on inorganic substrates, while solution-based sol-gel approaches are considered when thick films or nano-powders are desired. Also, lower equipment cost and reasonably good conformality of coatings may make sol-gel a low-cost alternative to CVD/ALD. However, the ALD approach may be required for the preparation of uniform conformal films on complex surfaces such as those with high aspect ratios.

Usually, the nature of the deposition process determines the way in which the thickness of the film is controlled. Thus, in conventional CVD, the film growth depends on the deposition time, while in ALD it is controlled by the number of deposition cycles.[1-3] In sol-gel processing, the films are created using two major approaches – spin coating or dip coating. In the first case, the substrate is spun at an angular speed ω and the precursor (sol) is directed onto its surface along the rotation axis. The thickness (h) of the created films depends on a complex combination of the sol's properties and the rotation speed of the substrate. In practice, they can be predicted using a semi-empirical formula

$$h = A\omega^{B}$$

where A and B are empirical coefficients. The dip coating process consists of the successive dipping and withdrawal of the substrate in and out of the solution. The thickness of the film obtained in one dipping-withdrawal cycle is determined[8] by the properties of the solution, i.e. viscosity (η), density (ρ), surface tension (σ) and the withdrawal speed (v) :

$$h = 0.945\{(v\eta)^{2/3}/ (g\rho)^{1/2}\sigma^{1/6}\}$$

While CVD/ALD techniques produce thin films of high uniformity and metal purity, sol-gel processing provides a unique and simple approach to tuning the film's chemical composition and morphology. Sol-gel processing can also offer a less expensive alternative to CVD/ALD, especially if in situ doping is required.

An example, when solution processing has been used successfully as an alternative to CVD/ALD was in the preparation of silicon thin-film transistors where the deposition of a polycrystalline silicon used a liquid precursor, cyclopentasilane (Si_5H_{10}).[9] The grain size in the films obtained were found to be as low as 300 nm, comparable to that for films typically prepared by CVD.

For questions, product data, or new product suggestions,
please contact the Materials Science team at matsci@sial.com.

Order: 1.800.325.3010 Technical Service: 1.800.231.8327
ALDRICH®

An illustration where CVD is clearly preferred over solvent-based processing, is the deposition of magnesium aluminum spinel ($MgAl_2O_4$). Magnesium aluminum spinel is an excellent material for refractory applications because of its mechanical strength, chemical resistance, and low density. Also, it shows potential as a humidity sensor and as a buffer layer for the growth of oxide superconductors. Thin films of $MgAl_2O_4$ have been successfully prepared by CVD using Mg-Al precursors such as $MgAl_2(OPr\text{-}i)_8$ or $MgAl_2(OBu\text{-}t)_8$. Sol-gel processing was employed for this application using a similar intermediate, $MgAl_2[(OCH_2CH_2)N]_3$, resulting in micro-porous powders.[10,11] Remarkably, certain groups of precursors, such as metal alkoxides, for example, can be used successfully in both CVD/ALD and Chemical Solution Deposition/Sol-Gel Processing of metal-oxide films and nano-structures.[12-14]

Thus, when used to the best of their abilities, Chemical Vapor and Solution Deposition techniques are excellent tools, to enable the design of a broad range of materials with pre-defined dimensions, morphology and properties.

Acknowledgements
I would like to thank Dr. S. Jasty, Dr.A.Korolev, Dr. M. Stender, and S. Adam for discussions and help in the preparation of the manuscript.

References:

(1) D.M. Dobkin and M.K. Zuraw, *Principles of Chemical Vapor Deposition: What's Going on Inside the Reactor*, **2003**, Kluwer Academic Publishers, Boston, Dodrecht, London. (2) R. Fischer, *Precursor Chemistry of Advanced Materials*, **2005**, Springer, New York. (3) D. Monsma, J. Becker, *Material Matters*, **2006**, Vol. 1, No. 3, 5. (4) S.K.Young's, *Material Matters*, **2006**, Vol 1., No. 3, 8. (5) F. Caruso, *Colloids and Colloid Assemblies: Synthesis, Modification, Organization, and Utilization of Colloid Particles*, **2004**, John Wiley & Sons, New York. (6) *Sol-Gel Technology for Thin Films, Fibers, Preforms, Electronics, and Specialty Shapes*, L.C. Klein, Ed., **1988,** Noyes Publ., Park Ridge, NJ. (7) A.C.Pierre, *Introduction to Sol-Gel Processing*, **2002** Kulwer Academic Publishers, Boston, Dodrecht, London. (8) V. Kiisk, *Optical Investigation of Metal-Oxide Films*, **2006**, Tartu University Press, Tartu. (9) T. Shimoda, Y. Matsuki, M. Furusawa, T. Aoki, I. Yudasaka, H. Tanaka, H. Iwasawa, D. Wang, M. Miyasaka, Y. Takeuchi, *Nature*, **2006**, *440*, 783. (10) K.F.Waldner, R.M.Laine, S. Dhumrongvaraporn, S.Tayaniphan, R.Narayanan, *Chem. Mater*. **1996**, *8*, 2850 (11) S.Mathur, M.Veith, T.Ruegamer, E.Hemmer, H.Shen, *Chem. Mater*. **2004**, *16*, 1304. (12) N. Lecerf, S. Mathur, H. Shen, M. Veith, S. Huefner, *Scripta Mater*. **2001**, *44*, 2157 (13) M. Veith, J. Chem. Soc., *Dalton Trans*., **2002**, 2405 (14) L.G. Hubert-Pfalzgraf, Inorg. *Chem. Communications* **2003**, *6*, 102.

High-Purity Metal Alkoxides

Metal	Precursor	Linear Formula	Purity (%)	Product No.
Aluminum	Aluminum isopropoxide	$Al[OCH(CH_3)_2]_3$	99.99	**229407-10G** **229407-50G** **229407-250G**
	Aluminum-tri-sec-butoxide	$Al[OCH(CH_3)C_2H_5]_3$	99.99	**511609-5G**
Germanium	Germanium(IV) ethoxide	$Ge(OC_2H_5)_4$	99.95	**339180-1G** **339180-5G** **339180-25G**
Hafnium	Hafnium(IV) n-butoxide		99	**667943-25G**
	Tetrakis(1-methoxy-2-methyl-2 propoxy)hafnium(IV)	$Hf(OC(CH_3)_2CH_2OCH_3)_4$	99.99	**568171-10G** **568171-25G**
Magnesium	Magnesium ethoxide	$Mg(OC_2H_5)_2$	98	**291846-5G** **291846-100G**
Niobium	Niobium(V) ethoxide	$Nb(OCH_2CH_3)_5$	99.95	**339202-5G** **339202-50G**
Tin	Tin(IV) *tert*-butoxide	$Sn(OC(CH_3)_3)_4$	99.99	**494135-5G** **494135-25G**
Tantalum	Tantalum(V) ethoxide	$Ta(OC_2H_5)_5$	99.98	**339113-10G** **339113-100G**
Titanum	Titanium(IV) isopropoxide	$Ti[OCH(CH_3)_2]_4$	99.999	**377996-5ML** **377996-25ML** **377996-100ML**
	Titanium(IV) methoxide	$Ti(OCH_3)_4$	99.99	**463582-25G**
Tungsten	Tungsten(VI) ethoxide		99	**667935-2G** **667935-10G**
Zirconium	Zirconium(IV) diisopropoxidebis(2,2,6,6-tetramethyl-3,5-heptanedionate)	$Zr(OCC(CH_3)_3CHCOC\text{-}(CH_3)_3)_2(OC_3H_7)_2$	99.99	**494151-5G** **494151-25G**
	Zirconium(IV) isopropoxide isopropanol complex	$Zr(OCH(CH_3)_2)_4 \cdot (CH_3)_2CHOH$	99.9	**339237-10G** **339237-50G**
	Zirconium(IV) *tert*-butoxide electronic grade	$Zr[OC(CH_3)_3]_4$	99.999	**560030-5G** **560030-25G**

The Savannah ALD System - An Excellent Tool for Atomic Layer Deposition

Dr. Douwe Monsma and
Dr. Jill Becker

Cambridge
NanoTech Inc.

Introduction

Atomic Layer Deposition (ALD) is a coating technology that allows perfectly conformal deposition onto complex 3D surfaces. The reason for this uniform coating lies in the saturative chemisorption of sequential cycles of precursor vapors. The process is illustrated in **Figure 1**. In **Figure 1a,** a silicon surface is terminated with hydroxyl groups (formed during contact with air). The wafer is inserted in an ALD reactor and a first precursor is introduced (here trimethyl aluminum, TMA, **Figure 1a-b**) using a fast pulse valve to a cylinder with liquid TMA. The precursor reacts with the surface layer, but not with itself, forming a single saturated monolayer. Subsequently, the TMA vapor and methane reaction products are pumped away and water vapor is introduced (**Figure 1c-d**). This forms a saturated monolayer of oxygen (**Figure 1e**) with a volatile reaction product of methane (again a saturated monolayer because the water molecules don't react anymore after the water formed the hydroxyl (OH) passivated surface). The methane and water are pumped away and the cycle is repeated until the desired coating thickness is obtained (**Figure 1f**).

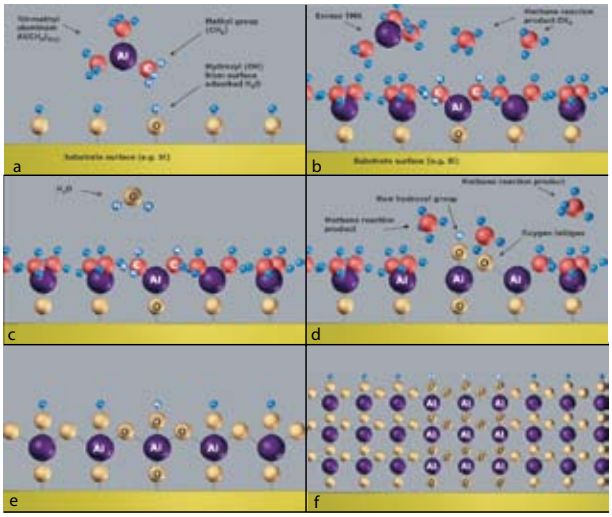

Figure 1a-f. Atomic Layer Deposition reaction cycle showing the formation of Al_2O_3 coating using trimethylaluminum (TMA) and water as precursors, and methane as volatile reaction product.

Since the films saturate to a monolayer with each precursor pulse, the coating will be equally thick inside small pores as on the surface of a substrate. This allows deposition inside photonic crystals, DRAM capacitor trenches, around suspended MEMS structures, around particles, etc. In fact, aspect ratios larger than 1:1000 can be routinely achieved using Cambridge NanoTech ALD systems; an example is shown in **Figure 2** where a uniform coating is formed inside 50 nm dia, 50 micron deep pores in anodically etched aluminum oxide substrates and in **Figure 3** where semiconductor nanowires have been coated conformally. For microelectronic applications, we have demonstrated lift-off of ALD coatings with nanometer resolution (**Figure 4**). Here we either used optical resist or e-beam resist to form patterned ALD coatings on silicon wafers. Dielectric and electronic properties have been tested using metal-insulator-metal capacitors. Dielectric constant and breakdown values for Al_2O_3, HfO_2 and ZrO_2 are listed in **Table 1**.

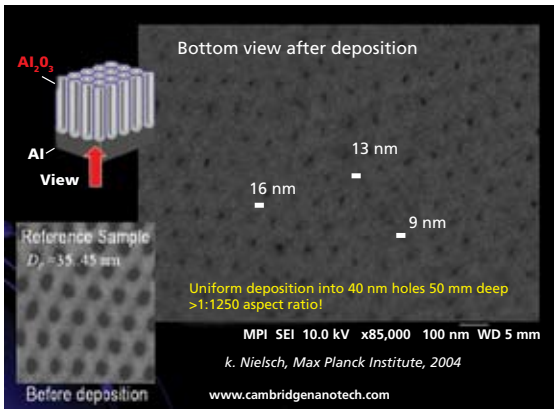

Figure 2. Conformal coatings inside anodic aluminum oxide substrates, with pores 50 microns deep conformally reduced in diameter from 40 nm to 20 nm, using Cambridge NanoTech ALD Systems.

The intrinsic deposition uniformity is an advantage for the ALD systems despite variability in process conditions. The deposition is relatively insensitive to variations of precursor flux over the substrate. In fact, usually overdosing is used to reach complete saturation, as well as to temperature variations. This makes ALD more repeatable and user friendly than chemical vapor deposition (CVD) or sputtering, where the thickness needs to be tracked constantly with a thickness monitor. Scaling is a further advantage of ALD. Batch reactors can be used where many substrates are stacked with small separations. All substrates can be coated at once with great uniformity. This in contrast to CVD where uniformity is compromised in batch systems, or sputtering where continuous line of sight with the sputter target is needed and batches are limited to only a couple of substrates, and very large targets and vacuum chambers are required.

Order: 1.800.325.3010 Technical Service: 1.800.231.8327

ALDRICH®

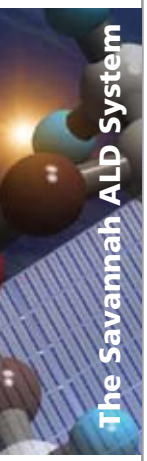

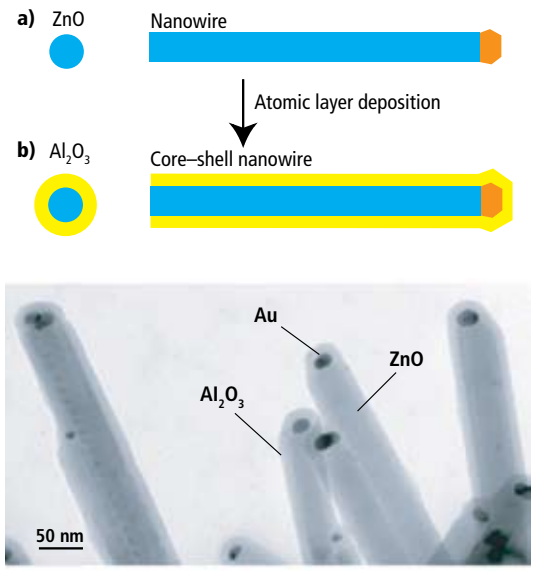

Figure 3. Conformal coatings around semiconductor nanowires using Cambridge NanoTech ALD systems.[2]

To summarize the advantages of ALD:

- Thickness is determined simply by number of deposition cycles.
- Precursors are saturatively chemisorbed, which results in stoichiometric films with large area uniformity and 3D conformality.
- Relatively insensitive to dust (film grows underneath dust particles).
- Intrinsic deposition uniformity and small source size, implies easy scaling.
- Nanolaminates and mixed oxides are possible.
- Low temperature deposition is possible (RT-400C).
- Gentle deposition process for sensitive substrates.

Because of the active synthesis of ALD precursors by chemists, the number of materials that can be deposited is increasing rapidly, and with it the number of applications is mounting.

The Savannah ALD System

The Savannah ALD systems manufactured by Cambridge NanoTech Inc. have unique features not found in other ALD systems. The reactor volume is low, allowing fast cycle times and very little precursor consumption. This in turn permits the use of a smaller vacuum pump and small precursor cylinders, mounted underneath the reactor. The footprint of this ALD system is consequently the smallest on the market (typically only 20"×20"). Despite its small size, substrates up to 200 mm can be deposited (Savannah 200 Model) with thickness uniformity and repeatability generally <+/-1% (Al_2O_3). With special lids, the height of the reactor can be modified to allow thick substrates and larger parts. Using a modular heated manifold, up to 6 precursors can be mounted, including solid, liquid, and gas precursors. All precursor heating is standard. Special 3-way ALD valves are employed that can be heated up to 200C, allowing a wide range of liquid and solid precursors to be used. The unique stop valve exposure mode allows deposition into narrow and deep pores, with aspect ratios larger than 1:1000 readily achieved.

The Savannah models have been outfitted in glovebox environments, allowing deposition onto air-sensitive substrates such as organic flat panel displays. In addition to the standard Savannah models, Cambridge NanoTech Inc. manufactures custom ALD systems for any substrate size. The Savannah models run in industrial and academic environments, both for specific R&D and general cleanroom use.

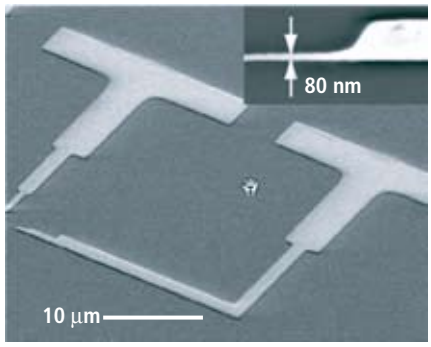

Figure 4. ALD Lift-off of various dielectric coatings using photoresist and e-beam resist with nanometer resolution.

Table 1. Properties of several high-κ materials grown using the same low-temperature ALD process as used for lift-off, measured at 20 K and room temperature (T_m).

Material	d (nm)	T_m	E_{BD} (MV/cm)	κ	Q_{BD} (mC/cm-2)
Al_2O_3	2.5	RT	8	9	6.4
Al_2O_3	10	RT	8.3	8.8	6.5
Al_2O_3	25	RT	8.2	8.2	6.0
Al_2O_3	50	RT	7.6	8.9	6.0
ZrO_2	25	RT	5.6	20	9.9
ZrO_2	100	RT	6	29	15.5
ZrO_2	50	20 K	8.2	29	21
ZrO_2	100	20 K	9.5	26	22
HfO_2	10	RT	6.5	17	9.7
HfO_2	25	RT	7.4	18.5	12
HfO_2	25	20 K	8.4	16.3	12.1

*Breakdown field, EBD=VBD/d (VBD is breakdown voltage, d is film thickness), dielectric constant k, and charge density at breakdown, QBD=CVBD.

Applications and Materials for ALD

In the field of micro- and nano-electronics, high-k dielectrics (Al_2O_3, HfO_2, ZrO_2, PrxAylOz, Ta_2O_5, La_2O_3), conductive gate electrodes (Ir, Pt, Ru, TiN) and metal interconnects (Cu, WN, TaN, Ru, Ir) have been applied. In particular, deposition onto semiconductors that do not form native oxides (such as SiO_2) ALD has been proven essential.

Because of its ability to coat conformally around rough and particulate surfaces, catalytic coatings form an important field of application for ALD. For example, coatings inside filters, membranes, catalysts (thin economical Pt for automobile catalytic converters), and ion exchange coatings in fuel cells (Pt, Ir, Co, TiO_2, V_2O_5).

Other important field of application are micro-electro-mechanical and nano-electromechanical systems (MEMS and NEMS). Here, suspended and 3D etched structures can easily be coated conformally using ALD. The same is true for biomedical devices, that often have complex shapes and can be coated with a variety of nitride ceramics.

TO ORDER: Contact your local Sigma-Aldrich office (see back cover),
call 1-800-325-3010 (USA), or visit sigma-aldrich.com/matsci.

In the field of optics, large improvements in uniformity of optical parameters and thickness can be obtained by using ALD. In addition, substrates don't need to be rotated to be coated all over and batch processes can be applied to reduce cost. Several fields of optics benefit from ALD: nanophotonics, solar cells, integrated optics, lasers, variable dielectric constant nanolaminates, Fabry-Perot, Rugate, flip-flop optical filters, and anti-reflection coatings (Al_2O_3, ZnS, SnO_2, Ta_2O_5, AlTiO, SnO_2, ZnO). For photonic crystals and inverted opals, ALD is conveniently the only technique that can be used to internal coatings.

ALD is commercially used in the fabrication of magnetic read heads (for insulating layers, mainly Al_2O_3) as well as for flat panel displays. More recently, ALD has proven to create excellent humidity barriers for organic light emitting displays (OLEDs).

Several niche applications have been found as well, such as piezoelectric layers (ZnO, AlN, ZnS), transparent electrical conductors (ZnO:Al, ITO) and gas/pH sensors (SnO_2, Ta_2O_5), wear, solid lubricant and corrosion inhibiting layers (Al_2O_3, ZrO_2, WS_2).

Besides many ceramics, ALD can now also deposit various metals, such as Ru, Pd, Ir, Pt, Rh, Co, Cu, Fe, and Ni, increasing the number of applications and advancing science by allowing precision coatings in places where no other technique has gone before.

References:
(1) K. Nielsch, Max Planck Institute, Germany, private communication. (2) Hongjin Fan, *Nature Materials* online, July **2006**, 1. (3) Biercuk et al. *Appl. Phys. Lett.* **2003**, *83*, 2405.

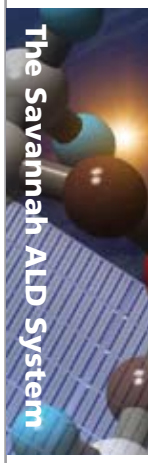

Volatile Precursors for Savannah ALD System*

Metal	Precursor	Linear Formula	Physical State	Product No.
Aluminum	Trimethylaluminum TMA	$Al(CH_3)_3$	Liquid, pyrophoric	**663301-25G**
Hafnium	Tetrakis(dimethylamido)hafnium(IV) TDMAH	$Hf[N(CH_3)_2]_4$	Solid, air-sensitive	**666610-25G**
Ruthenium	Bis(Ethylcyclopentadienyl)ruthenium(LI)	$Ru(C_5H_4\text{-}C_2H_5)_2$	Liquid	**679798-10G**
Tantalum	Tris(diethylamido)(*tert*-butylimido)-tantalum(V)	$(CH_3)_3CN{=}Ta(N(C_2H_5)_2)_3$	Liquid, air-sensitive	**668990-10G**
Titanium	Tetrakis(dimethylamido)titanium(IV) TDMAT	$Ti[N(CH_3)_2]_4$	Liquid, air-sensitive	**669008-25G**
Tungsten	Bis(*tert*-butylimino)bis(dimethylamino)tungsten(VI)	$((CH_3)_3CN)_2W(N(CH_3)_2)_2$	Liquid, air-sensitive	**668885-10G**
Zinc	Diethylzinc	$Zn(C_2H_5)_2$	Liquid, pyrophoric	**668729-25G**
Zirconium	Tetrakis(dimethylamido)zirconium(IV) TDMAZ	$Zr[N(CH_3)_2]_4$	Solid, air-sensitive	**669016-25G**

*Packaged in steel cylinders specially configured for use with the Savannah ALD system.

For a complete list of metal precursors for CVD/ALD, visit sigma-aldrich.com/precursors.

Spend Your Time Getting ALD Results

Affordable, Fast and Versatile
Stand-Alone Atomic Layer Deposition System for Your Lab

Sigma-Aldrich and our exclusive partner, Cambridge NanoTech Inc., are pleased to present an **EASY TO USE** stand-alone ALD system for your research in:

Substrate Size ..... up to 4-in wafers and up to 8-in wafers
Substrate Temperature ..... 25–400 °C; ±0.2 °C
Precursor Sources ..... 2, heated
Deposition Uniformity ..... <1%
Footprint ..... 500 × 550 mm
Deposition ..... High speed/high aspect ratio
Cleanroom Compatibility ..... Class 100

Turnkey Yet Client Customizable

The standard tool comes complete with vacuum system and Lab-View/PC control and is CUSTOMIZABLE to your specifications. **Plus,** Sigma-Aldrich will help you get the materials and precursors you need to make your project a success!

To learn more about this system, visit sigma-aldrich.com/matsci or email **matsci@sial.com** and a representative will contact you with more details.

Order: 1.800.325.3010 Technical Service: 1.800.231.8327
ALDRICH®

Sol-Gel Science for Ceramic Materials

Dr. Sandra Kay Young
US Army Research Laboratory

Introduction

Silicon-based research has drawn much attention in recent years with targeted organizations such as the *International Sol-Gel Society* hosting workshops,[1] and the *Sol-Gel Gateway*[2] hosting a compendium of information regarding the sol-gel field including conference information. In addition, peer-reviewed journals such as *Journal of Sol-Gel Science and Technology, Chemistry of Materials, and Journal of Non-Crystalline Solids* publish a significant number of articles that focus on silicon-based materials. These organizations, conferences, and journals highlight much of the major silicon-based research generated in academia and industry. Research involving reactive silicone chemistry has focused on the production of pure silicon and hybrid materials, hydrosilylation, ring-opening and atom transfer polymerizations, polymerizations with controlled stereochemistry, and condensation reactions. Reactions with silicones produce a wide range of materials that encompass the major areas of silicon chemistry: polymers, elastomers, ceramics, interpenetrating networks, reinforcing fillers, membranes, microlithography, photoinitiation, high performance polymers, and sol-gel-derived ceramic precursors.

While it was known earlier, sol-gel chemistry has been investigated extensively since the mid-1970's, when sol-gel reactions were shown to produce a variety of inorganic networks that can be formed from metal alkoxide solutions.[3] Through sol-gel processing, homogeneous, high-purity inorganic oxide glasses can be made at ambient temperatures rather than at the very high temperatures required in conventional approaches. Various products, such as molded gels,[4,5] spun fibers,[6,7] thin films,[8-10] molecular cages,[11,12] and xerogels[13] have been developed for utility in such areas as gas separations, elastomers, coatings, and laminates. It is through the inorganic component incorporation into organic polymers that a wide variety of desired property modifications can be achieved.

The precursors used in sol-gel processing consist of a metal or metalloid element surrounded by various reactive ligands. Metal alkoxides, such as aluminates, titanates and zirconates, are the most popular precursors because of their high reactivity towards water. The most widely used non-metal alkoxides are alkoxysilanes, such as tetramethoxysilane (TMOS, Aldrich Prod. No. **679259**) and tetraethoxysilane (TEOS, Aldrich Prod. No. **333859**). Although ethyl groups are the most common alkoxy groups, methoxy, propoxy, butoxy and other long-chain hydrocarbon alkoxy groups are also used in alkoxysilanes. Metal alkoxides are commonly used in the sol-gel process either alone or in combination with non-metal alkoxides such as TEOS or alkoxyborates.

Sol-Gel

The sol-gel process consists of a series of hydrolysis and condensation reactions of an alkoxide, which proceed according to the reaction scheme shown in **Figure 1**. Here, alkoxysilanes are used as an example but all of the metal alkoxides react similarly. Hydrolysis is initiated by the addition of water to the silane solution under acidic, neutral, or basic conditions.

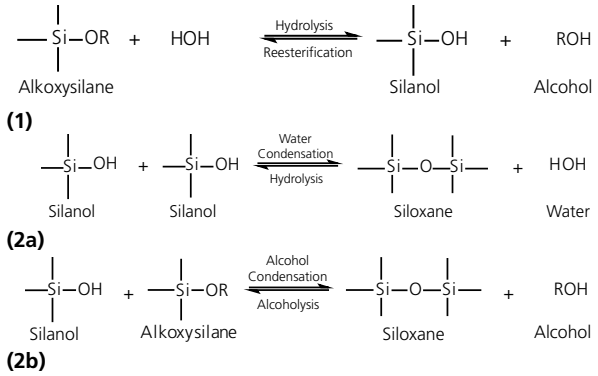

Figure 1. Sol-Gel Reaction Scheme.

While hydrolysis and condensation reactions of most metal alkoxides can be carried out without catalyst because of the extremely fast rates of reaction, alkoxysilanes hydrolyze much more slowly, requiring the addition of either an acidic or basic catalyst. In order to slow down the reaction kinetics of the metal alkoxides, Drying Chemical Control Additives (DCCAs) are often used.14,15 These include tetrahydrofuran, formamide, dimethylformamide, and oxalic acid. DCCAs slow down the reaction kinetics by forming hydrogen bonds with the intermediates in the reaction. The DCCA solvent can be removed by evaporation in order to allow the reaction to progress.

Benefits and Utility

Sol-gel processing is beneficial in the formation of ceramic and glass films for many reasons. It is a simple reaction that does not require exotic materials, catalysts or expensive deposition equipment. Likewise, sol-gel reactions do not employ extreme reaction conditions. The reactions take place at room temperature and require only moderate temperatures to 'cure' the gel, removing the water/alcohol that the reaction generates. The properties of the materials prepared using sol-gel approaches are easy to modify by utilizing an organically modified alkoxide or a variable arm metalloid (for example, an alkoxyborate instead of an alkoxysilane).

Sol-gel processing is commonly used to modify S2 glass fibers (a type of high performance fiberglass) used in composites. Coating glass surfaces with a sol-gel film helps the glass gain strength and resists shattering. Also, sol-gel materials have been used in composites to reinforce existing polymeric structures, such as polyesters,[16] Nafion®,[17] Surlyn®.[18] In all of these applications, sol-gel alkoxysilanes and alkoxytitanates were used as received with a purity of 97% or greater.

TO ORDER: Contact your local Sigma-Aldrich office (see back cover),
call 1-800-325-3010 (USA), or visit sigma-aldrich.com/matsci.

Modifing the Sol-Gel Network

A convenient way to modify ceramic and composite materials, such as those referred to in the previous paragraph is through the use of Organically Modified Silicates (ORMOSILs). ORMOSILs are derived from tetrafunctional silicon alkoxides such as TEOS, as shown in **Figure 2**, where **n** is representative of the number of organic moieties connected to the silicon atom and **f** is representative of the number of reactive alkoxy groups connected to the silicon. **R**, **R**′, and **R**″ are the functional group(s) on an organically modified silicate such as methyl, vinyl, or benzyl. Often, the organic moiety includes a reactive group such as an amine or epoxide, which makes possible subsequent reactions.

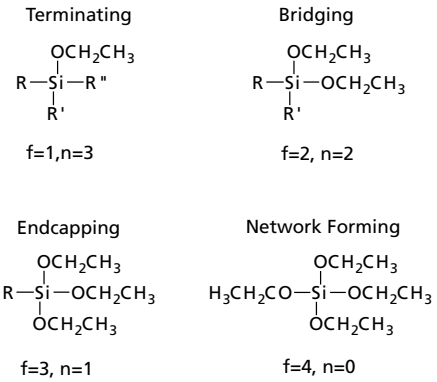

Figure 2. Functionality of ORMOSILs

Silsesquioxanes are other widely used inorganic-organic modifiers in ceramic and composite materials. Bridging silsesquioxanes (**Figure 3**) contain a substituent (**R**) that is hydrocarbon based but can also contain organic spacer functionalities. Since silsesquioxanes are often incorporated into polymer systems, the R-group should be as similar as possible to the repeat unit thus increasing interface compatibility.

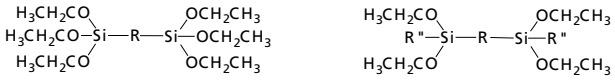

Figure 3. Examples of a 6-arm and a 4-arm Bridging Silsesquioxane.

In addition, numerous caged structures are being incorporated into ceramic and composite materials through sol-gel chemistries. These structures, such as polyhedral silsesquioxanes[19,20] (also commonly known as PSS) or zeolites,[21] add specific porosity and rigidity to the material. Caged structures can be incorporated through non-covalent (trapping the material within the ceramic structure) or covalent bonding.

Studying Sol-Gel Networks

Sol-gel bonding in ceramic and composite structures is often studied through FTIR and solid-state NMR (^{29}Si MAS NMR for example). Elemental ratios can be determined via XPS for surfaces and through prompt γ neutron activation analysis for bulk materials. **Figure 4** shows FT-IR data from a sol-gel ORMOSIL of tetraethylorthosilicate (T):diethoxydimethylsilane (D) sol-gels polymerized within a Nafion structure delineating different silicon bond structures.[22] The prominent absorbance is due to the asym metric Si-O-Si envelope, consisting of both the cyclic (~1080 cm-1) and linear (~1030 cm-1) components.

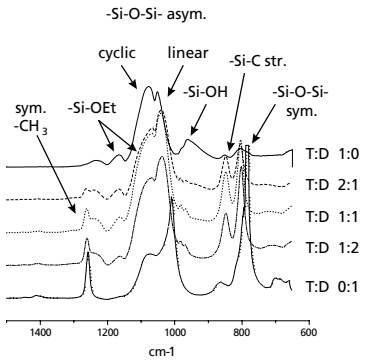

Figure 4. FT-IR ATR Difference Spectra for Tetraethylorthosilicate (T): Diethoxydimethylsilane (D) sol-gels polymerized within a Nafion structure.[22]

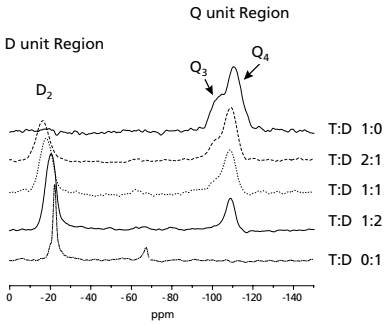

Figure 5. Shows solid-state ^{29}Si MAS NMR data from ORMOSIL tetraethylorthosilicate/diethoxydimethylsilane polymerized within a Nafion structure delineating different silicon bond structures.[17,21]

Conclusion

Sol-gel science and technology have the potential to make a significant impact in modification of the properties of materials. One of the most significant benefits of sol-gel science is its use of room temperature conditions and insensitivity to the atmosphere. These features will allow its use with various materials that cannot tolerate high temperatures, and does not limit the researcher to using special equipment, such as a dry box.

References:

(1) www.isgs.org (2) www.solgel.com
(3) Nogami, M. et al. *J Non-Cryst Solids* **1980**, *37*, 191.
(4) Wei, Y. et al. *J Sol-Gel Sci & Tech* **1996**, *7*, 191.
(5) Mackenzie, J. D. *J Non-Cryst Solids* 1982, *48*, 1. (6) Mascia, L. et al. *Composites Part A* **1996**, 27A (12),1211. (7) Sakka, S. et al. *J Non-Cryst Solids* **1986**, *82*, 24. (8) Brinker, C. J. et al. *J Memb Sci* **1994**, *94*, 85. (9) Yoldas, B. E. *J Non-Cryst Solids* **1989**, *112*, 419. (10) Schmidt, H. *J Non-Cryst Solids* **1980**, *37*, 191. (11) Zusman, R. et al. *Anal Biochem* **1992**, *201*, 103. (12) Yakubovich, T. N. et al. *Russian J Coord Chem* **1994**, *20* (10), 761. (13) Hobson, S. T. et al. *Chem Mat* **1997**, *9*, 616. (14) Brinker, C. J. *J Non-Cryst Solids* **1988**, *100*, 31. (15) Hench, L. L. et al. *Chem Rev* **1990**, *90*, 33. (16) Young, S. K. et al. *Polymer* **2002**, *43*, 6101. (17) Young, S. K. et al. *Poly. Eng. & Sci.* **2001**, *41* (9), 1529. (18) Siuzdak, D.A. et al. *J Poly Sci Part B-Polym Phy* **2003**, *41*(1),11. (19) Shea, K. et al. J Am Chem Soc **1992**, *114*, 6700. (20) ChemFiles **2001**, Vol. 1, No. 6. (21) Cot, L. et al. *Solid State Sci* **2000**, *2*, 313. (22) Young, S. K. *Organic-Inorganic Composite Materials: Molecular Tailoring of Structure-Property Relationships* PhD Thesis **1999**.

Order: 1.800.325.3010 Technical Service: 1.800.231.8327
ALDRICH®

Silane Precursors

For unit sizes and prices of products below, please visit sigma-aldrich.com.

Tri(methoxy)silanes

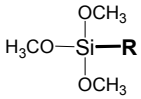

440175 (95%)	**435643** (>97%)	**235758** (98%)	**104744** (98%)
438340 (98%)	**91877** (97%)	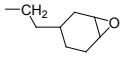 **413321** (98%)	**440183** (>97%)
18265 (97%)	**175617** (95%)	**281778** (97%)	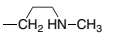 **551635** (97%)
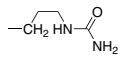 **440817** (97%)	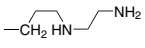 **104884** (97%)	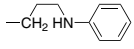 **440809** (97%)	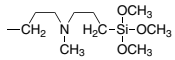 **555150** (97%)
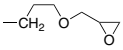 **440167** (98%)	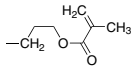 **440159** (98%)	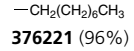 **376221** (96%)	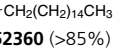 **52360** (>85%)
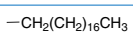 **376213** (90%)			

Tri(ethoxy)Silanes

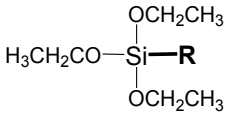

391042 (96%)	**539317** (97%)	**435678** (98%)	**29262** (>97%)
A36301 (97%)	**125377** (97%)	**10160** (>97%)	**435686** (95%)
440140 (99%)	**374156** (98%)	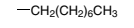 **440213** (>96%)	**667420** (98%)
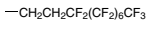 **658758** (97%)	**44237** (>95%)		

Other Alkoxysilanes

253006 (99%)	**254371** (98%)	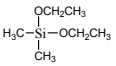 **175595** (97%)	**446203** (97%)
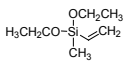 **259462** (99%)	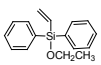 **484319** (97%)	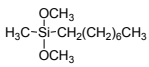 **68215** (>95%)	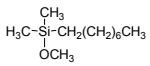 **375977** (98%)
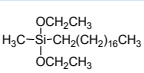 **452793** (95%)	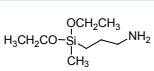 **371890** (97%)	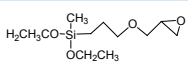 **435171** (97%)	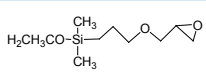 **539260** (97%)
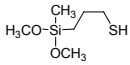 **446173** (95%)	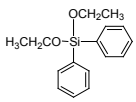 **D83532** (97%)		

TO ORDER: Contact your local Sigma-Aldrich office (see back cover), call 1-800-325-3010 (USA), or visit sigma-aldrich.com/matsci.

Development of a Hermetic Barrier Using Vinyl Triethoxysilane (VTEOS) and Sol-Gel Processing

Ariel Jackson, and
Dr. Andrei Jitianu,
Professor Lisa C. Klein

Department of Materials Science and Engineering, Rutgers University

Introduction

Humidity barriers are an essential part of microelectronics, micro-electromechanical systems (MEMS) and displays using organic-light emitting diodes (OLEDs). These barriers are required to have low processing temperatures. Hybrid organic-inorganic barrier materials can be applied in a sol-gel process at low temperature, in order to provide hermeticity. The inorganic content is designed to be the barrier, while the hydrophobic, organic content repels water and fills porosity.

Our goal is to develop hermetic barriers for electronics and electrochemical devices. The barrier has to prevent water, water vapor, and gases from permeating the coating and reacting with the device. Many low temperature hybrids have been synthesized using the sol-gel process and methacrylate compounds.[1,2] Other hybrids have been discussed in detail.[3,4] The concept is that the sol-gel process produces an oxide at low temperatures. Specifically, the process is used to produce silica, either as a network or as an agglomeration of nano-sized particles. The hybrid approach incorporates an organic component with the oxide, by either simultaneously or sequentially polymerizing the organic along with the inorganic component.

Typically, the inorganic component is derived from the hydrolysis and condensation polymerization of tetraethyl orthosilicate (TEOS, Aldrich Prod. No. **333859**) to form a network of silica, containing bridging oxygens. In this study, we use vinyl triethoxysilane (VTEOS, Aldrich Prod. No. **679275**) to generate an oxide network with polymerizable vinyl groups. In this case, the advantage of VTEOS over TEOS is the presence of an inorganic and organic network.

We analyzed the effectiveness of VTEOS in creating a hydrophobic barrier and how ultraviolet (UV) irradiation affected the VTEOS system. The properties of the films were investigated, and contact angle measurements were made to assess hydrophobicity.

Synthesis Method

The flowchart for synthesizing barrier coatings is shown in **Figure 1**. First the precursor, vinyl triethoxysilane (VTEOS), was mixed with the solvent ethylene glycol mono-butyl ether (EGMBE). Deionized water and acetic acid (CH_3COOH) were added and the solution was stirred for 20 hours. The initiator was benzoyl peroxide (BPO) for free-radical polymerization (0.1 wt %). Once the initiator was added, the solution was stirred for 4 hours before microscope slides and stainless steel coupons were dipped into the solution. A dip coater with a screw drive was used to lower and raise the slide.

The films were allowed to dry over night at room temperature before heating to 70 °C for 30 minutes. UV irradiation was carried out, followed by a wash in NaOH to remove excess BPO. Finally, the samples were dried and evaluated.

Uniform films were obtained on both glass and stainless steel substrates. Contact angle measurements were acquired using deionized water and calculated using KSV CAM Optical Contact Angle with Pendant Drop Surface Tension Software 3.80. The AFM images were acquired in a contact mode using a Nanoscope IV Scanning probe microscope Veeco™.

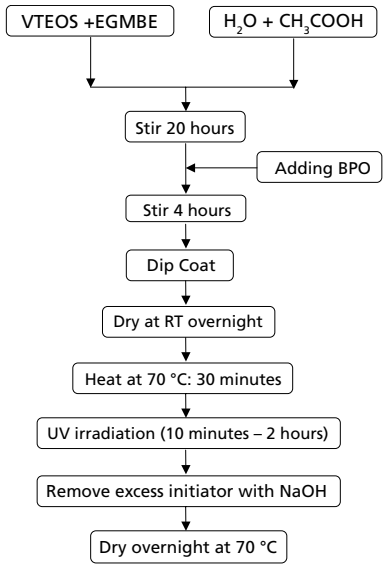

Figure 1. Flow chart of the synthesis of hybrid coatings using VTEOS via a sol-gel process.

Results and Discussion

Two samples are compared. One coating was prepared with four moles of water to one mole of VTEOS and the other one with six moles of water to one mole of VTEOS. Four moles is commonly said to be the stoichiometric water to hydrolyze a tetrafunctional silane, making six moles an excess. This assumes that one mole of water hydrolyzes each ethoxy group, although some condensation polymerization often accompanies further hydrolysis.

The results of the contact angle measurement are shown in **Figures 2a and 2b**. In Figure 2a, the contact angle for the drop of water on the coating prepared with four moles of water is 90.5°. For the sample that used six moles of water, the measured contact angle is 118.4°. This angle is much greater than 90°, and the coating is clearly super-hydrophobic.

Order: 1.800.325.3010 Technical Service: 1.800.231.8327

ALDRICH®

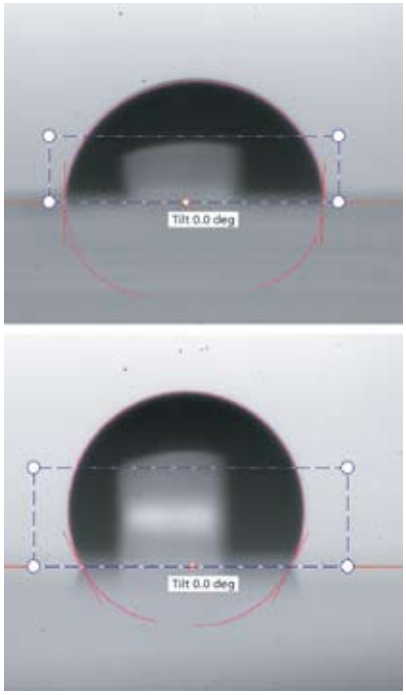

Figure 2a. Contact angle θ, for coating prepared using four moles H_2O: θ = 90.5°.

Figure 2b. Contact angle θ, for coating prepared using six moles H_2O: θ = 118.4°.

While samples appeared visually uniform, the AFM scans revealed the surface morphology. The surface roughness for the sample prepared with four moles of water was about 4.71 nm, as shown in **Figure 3**. The surface roughness adds to the hydrophobicity through the so-called lotus effect.

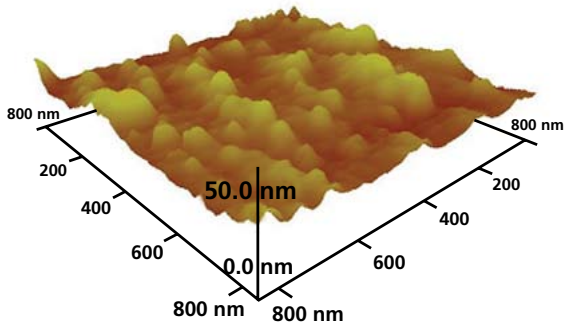

Figure 3. AFM image of surface of coating prepared with four moles H_2O, showing an average roughness of 4.71 nm.

The vinyl groups were found to be on the surface of the coatings, as measured by Attenuated Total Reflectance-Fourier Transform Infrared Spectroscopy(ATR-FTIR spectrum not shown). Further analyses of the spectra are in progress. A schematic of the polymerization of the vinyl groups on the surface is shown in **Figure 4.** More studies of the surface polymerization are underway.

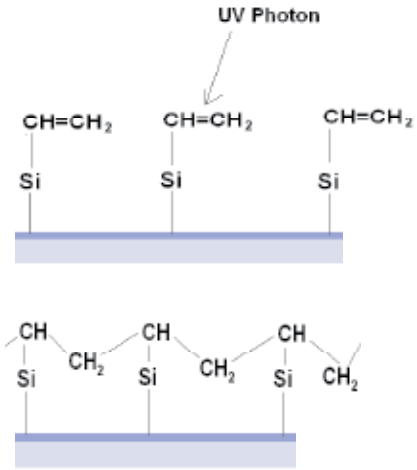

Figure 4. Schematic of photopolymerization of the vinyl groups of VTEOS-derived coatings.

Conclusions

Hybrid coatings have been prepared by the sol-gel process starting with VTEOS. The surfaces are hydrophobic, with the coating prepared with six moles of water showing a contact angle of 118.4°. The super-hydrophobicity is explained by the roughness of the surface on the nanoscale and by the presence of vinyl groups on the surface. We propose that the simultaneous generation of the two networks, inorganic by a sol-gel process and organic by photopolymerization, is a useful route to hydrophobic, dense, low temperature coatings for hermetic applications.

References

(1) A. B. Wojcik, L. C. Klein, *J. Sol-Gel Science and Technology,* **1995**,*4*, 57. (2) A.B. Wojcik, L. C. Klein, *J. Sol-Gel Science and Technology* **1995**, *5*,77. (3) A. B. Wojcik, L. C. Klein, *Appl. Organometallic Chem.* **1997**, *11*,129. (4) D. Avnir, L. C. Klein, D. Levy, U. Schubert, *A. B. Wojcik, The Chemistry of Organosilicon Compounds Vol. 2*, Eds. Z. Rappoport, Y. Apeloig, **1998**, Wiley, London, p. 2317.

For more information on
Volatile Precursors for NanoFabrication
see *ChemFiles Vol 4. No 3* and, for more information on Silsesquioxanes see **Silsesquioxanes: Bridging the Gap between Polymers & Ceramics** *ChemFiles Vol. 1 No 6*.
Both publications are available in PDF format at
sigma-aldrich.com/mslit.

TO ORDER: Contact your local Sigma-Aldrich office (see back cover),
call 1-800-325-3010 (USA), or visit sigma-aldrich.com/matsci.

Deposition Grade Silanes for Sol-Gel Processing

Silane Precursor	Structure	Product No.
Allyltrimethoxysilane	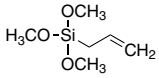	**679267-50G**
Butyltrichlorosilane	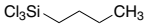	**679224-50G**
[3-(Diethylamino)propyl]trimethoxysilane	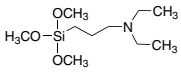	**679356-50G**
Ethyltrichlorosilane		**679216-50G**
Isobutyl(trimethoxy)silane		**679364-50G**
Methyltrichlorosilane	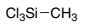	**679208-50G**
N-Propyltriethoxysilane	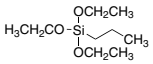	**679321-50G**
Pentyltrichlorosilane	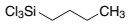	**679194-50G**
Tetramethyl orthosilicate	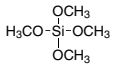	**679259-50G**
Tetrapropyl orthosilicate	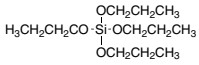	**679240-50G**
Triethoxy(octyl)silane	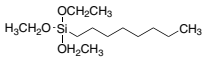	**679305-50G**
Triethoxyphenylsilane	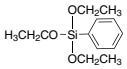	**679291-50G**
Triethoxyvinylsilane	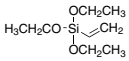	**679275-50G**
Trimethoxymethylsilane		**679232-50G**
Trimethoxyphenylsilane	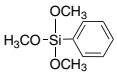	**679313-50G**

Purity of the above deposition-grade silanes is 98+% by chemical assay. Trace metals and impurity profiles are reported on the Certificate of Analysis.

For a complete list of precursors for Sol-Gel Processing, visit sigma-aldrich.com/solgel.

Order: 1.800.325.3010 Technical Service: 1.800.231.8327

ALDRICH®

Silicon-Based Passive and System-in-Package Integration: Options for Atomic Layer Deposition

Dr. Fred Roozeboom, NXP Semiconductors Research and Dr. Erwin Kessels, University of Technology, Eindhoven

In the past decade, the integration of passive components in silicon and the further 3D integration and stacking of individual chips from different technologies (e.g. CMOS, GaAs, MEMS) into one package ('heterogeneous' integration) have been developed to such an extent that now the first mass-volume production has begun. Today, the International Technology Roadmap for Semiconductors includes the future projections for the next generation Si-based Integrated Passives and System-in-Package integration.[1]

Recently, the first highly-integrated cellular RF transceiver systems based on the use of these technologies were launched.[2] Here, amongst others, Philips (now NXP) Semiconductors, utilizes back-end silicon processing to integrate passive components onto a silicon substrate that can act as a carrier for the heterogeneous integration of active component dies, MEMS dies, etc.[3] As an example, a transceiver IC can be flip-chip mounted onto this passive component silicon substrate, thus minimizing interconnect parasitics and the footprint area. This sub-assembly is then flipped back into a standard leadframe package (**Figure 1**).[3]

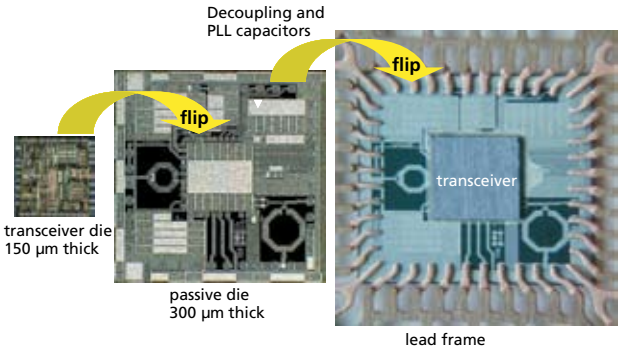

Figure 1. Passive die with active transceiver die flipped on top, double-flipped on a lead frame (left open, without moulding compound). This is an example of a Bluetooth System-in-Package 'plug and play' radio module. (From Ref. 3).

The passive die is made in the so-called PICS (Passive Integration Connecting Substrate) technology developed to integrate passive components such as high-Q inductors, resistors, accurate MIM capacitors and, in particular, high-density (~30 nF/mm^2) MOS 'trench' capacitors for decoupling and filtering. These are fabricated in silicon by dry-etching arrays of macropores with ~1.5 µm width and up to ~30 µm depth. Trench capacitors filled with ~ 30 nm silicon oxide and nitride ('ONO') dielectrics and a poly-Si/ Al top electrode showed superior dielectric breakdown voltage (30 V typical), very low leakage current, and long lifetime.[4,5]

A next miniaturization step includes the use of so-called high-k dielectrics (based on HfO_2, etc.) to compose MIS and MIM trench capacitors with increased capacitance densities of ≥200 nF/mm^2. One step towards System-in-Package is the etching and Cu-filling (electroplating) of viaholes of 10–200 µm widths and depths up to 300 µm. Vias are through-wafer holes filled with materials for heat spreading, electrical grounding and low-inductance signal interconnection from one wafer side to the other. This concept makes way for 3D die-stacking and generic System-in-Package integration with small form factor.

One of the major challenges in realizing high-density trench capacitors and in making through-wafer vias for 3D wafer and die stacking is to find an attractive pore lining and filling fabrication technology at reasonable cost and reaction rate as well as low temperature (for back-end processing freedom). The deposition for the insulating, dielectric, and performed at conductive layers (i.e. electrodes, seed layers and Cu-diffusion barriers) should be highly uniform and step-conformal and low-temperature (≤400 °C). Atomic Layer Deposition (ALD) is an enabling candidate here, by virtue of the self-limiting mechanism of this layer-by-layer deposition technique. A substrate surface is submitted to alternating exposures to vapors of two reagents, for example, trimethylaluminum (TMA) and water vapor in the case of Al_2O_3 deposition. Through its self-limiting surface reactions, ALD enables the uniform lining or filling of high aspect ratio pores with (sub)monolayer control. The self-limiting character provides inherent conformality, as demonstrated for even challenging devices like deep DRAM trench capacitors with ~60:1 aspect ratios at design rules below 100 nm.[6] Yet, ALD process improves the production of many other devices with a large topology, such as viaholes in stacked dies, MEMS, planar waveguides, multilayer optical filters, and layers protecting against diffusion, oxidation, corrosion, etc.

The application of ALD in trench capacitors and viaholes leads to additional challenges relative to flat wafers. For example, for the ALD of oxides the roughness on the trench sidewalls may cause undesired lower breakdown voltages. Also, the formation of interfacial oxide layers may lead to undesired low relative dielectric constants (cf. **Figure 2**). A proper pre-cleaning procedure (e.g. HF dipping, rinsing) is essential to minimize this. Furthermore, a proper uniform layer thickness and microstructure (morphology and texture) over the entire pore depth is necessary to achieve good insulating layers, and are certainly not obvious. Adsorption and desorption play an important role in filling and emptying the pores. In particular, at the given pressure and macropore dimensions the ALD process proceeds in a different diffusion regime (Knudsen diffusion) limiting the free diffusion of the gaseous ALD reagents and products. Timing of the cycling of the gases, including extended purging steps, needs to be optimized for additional adsorption and desorption processes of precursors.[7] Only then ideal nanolaminates can be achieved.

TO ORDER: Contact your local Sigma-Aldrich office (see back cover), call 1-800-325-3010 (USA), or visit sigma-aldrich.com/matsci.

For the deposition of conductive layers by ALD, for the application as electrodes, seed layers, diffusion barriers (e.g. against Cu-diffusion in vias) there is a substantial choice between thermal and plasma-assisted ALD. The plasma-based process can lead to improved material properties as has clearly been demonstrated by results on conductive TiN films.[8] The process based on $TiCl_4$ dosing in combination with H_2-N_2 plasma exposure has yielded thin TiN films with excellent resistivity and low impurity levels (C, H, Cl, etc.) greatly surpassing the material quality achieved with the thermal process employing NH_3 dosing. Moreover, in terms of acceptable material quality, the thermal process is limited to the substrate temperature range of 300–400 °C while the plasma-based process can yield fair material properties down to temperatures as low as 100 °C.

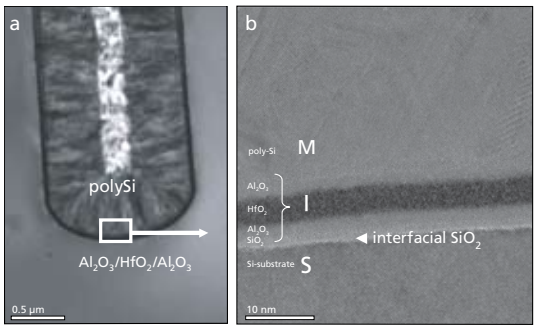

Figure 2. (a) SEM cross-section and (b) high-resolution TEM image of an $Al_2O_3/HfO_2/Al_2O_3$ dielectric layer stack, grown by thermal ALD with a poly-Si electrode layer on top.

TiN films deposited by plasma-assisted ALD for application as electrode materials in trench capacitors have already been explored (**Figure 3**). Another benefit from the plasma process is that tailoring the plasma composition and exposure time as shown for metal nitrides such as TiN and TaN can control the stoichiometry of the films. For example, for TaN deposited from metalorganic precursors (e.g., pentakisdimethyl aminotantalum) it is possible to tune the properties from insulating N-rich TaN by using a H_2-N_2 plasma, to low-resistivity TaN by using a relatively long H_2 plasma exposure, to very low resisitivity TaCN films with a large amount of carbon using a relatively short H_2 plasma exposure.

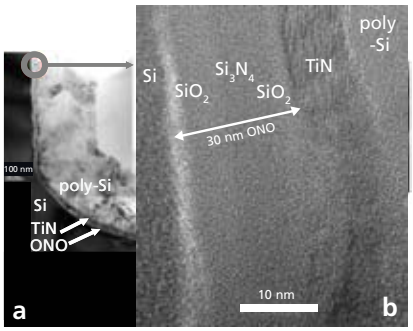

Figure 3. (a) SEM cross-section and (b) high-resolution TEM image of a MOS stack consisting of 30 nm 'ONO' dielectric and 10 nm plasma-assisted ALD TiN with 0.3 µm LPCVD grown poly-Si on top.

ALD is, in principle, ideal for depositing nanolaminate stacks, for example *oxide/nitride* multilayers used in trench capacitors. Multilayer stacks of 'high-k' dielectric layers (Al_2O_3, Ta_2O_5, HfO_2, etc.) and conductive layers (TiN, TaN) on wafers with a large topography enable MIM capacitors with ultrahigh capacitance density. A challenging example is given in **Figure 4**. The TEM images show the potential of ALD in growing multilayer stacks in high aspect ratio features. In our macropore arrays described above, a multilayer stack of 20 nm Al_2O_3 // 25 nm TiN // 20 nm Al_2O_3 // 25 nm TiN was deposited in 35 µm deep pores from $TiCl_4$ and NH_3 using thermal ALD. Here, the Al_2O_3 was grown from trimethylaluminum and O_3 plasma at 380 °C and the TiN was grown from $TiCl_4$ and NH_3 at 400 °C. It appeared that the layer thickness all along the pores was, within 10 % accuracy, 20 nm for the Al_2O_3 and 25 nm for TiN.

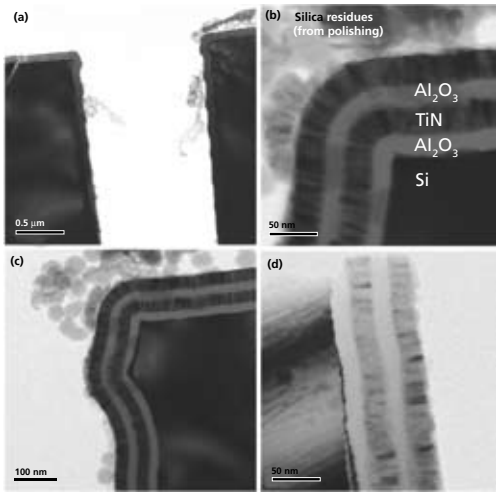

Figure 4. TEM images of a 20 nm Al_2O_3 // 25 nm TiN // 20 nm Al_2O_3 // 25 nm TiN multilayer grown in a pore with ~35 µm depth; **a)** overview image displaying both sides of one pore (top); **b)** and **c)** images at the upper part of the pore; **d)** image at ~25 µm pore depth. ALD performed by H.D. Kim, Jusung Engineering.

It can be concluded that the manufacturing of ultrahigh density (>200 nF/mm^2) capacitors is within reach and the same holds for growing seed layers for Cu-electroplating in viaholes and Cu-diffusion layers such as TaN. Thus there is a bright prospect for ALD in passive and heterogeneous integration, provided ALD is further developed to maturity and cost factors are reduced (e.g. development of batch ALD to compensate for low growth rates in single-wafer ALD). Also the development of low-temperature processing is important. This will be further facilitated by the availability of novel and dedicated precursor chemicals.

Silicon-Based Passive and System-in-Package

Order: 1.800.325.3010 Technical Service: 1.800.231.8327

ALDRICH®

For questions, product data, or new product suggestions,
please contact the Materials Science team at matsci@sial.com.

Acknowledgement

The technical contributions by J. Klootwijk, W. Dekkers and M. Kaiser (Philips) and S. Heil (TU Eindhoven) are gratefully acknowledged.

References

(1) ITRS Roadmap **2005** edition, *Assembly and Packaging*, see: www.itrs.net/Links/2005ITRS/Home2005.htm. (2) www.3d-ic.org/literature.html. (3) F. Roozeboom, A.L.A.M. Kemmeren, J.F.C. Verhoeven, F.C. van den Heuvel, J. Klootwijk, H. Kretschman, T. Frič, E.C.E. van Grunsven, S. Bardy, C. Bunel, D. Chevrie, F. LeCornec, S. Ledain, F. Murray and P. Philippe, *Thin Solid Films* **2006**, *504*, 391. (4) F.Roozeboom, A.Kemmeren, J.Verhoeven, F.van den Heuvel, H.Kretschman and T.Frič, *Mat. Res. Soc. Symp. Proc.* **2003**, *783*, 157. (5) F. Roozeboom, A.L.A.M. Kemmeren, J.F.C. Verhoeven, F.C. van den Heuvel, J. Klootwijk, H. Kretschman, T. Frič, E.C.E. van Grunsven, S. Bardy, C. Bunel, D. Chevrie, F. LeCornec, S. Ledain, F. Murray and P. Philippe, *Electrochem. Soc. Symp. Proc.* **2005**, *2005*,16. (6) M. Gutsche, H. Seidl, J. Luetzen, A. Birner, T. Hecht, S. Jakschik, M. Kerber, M. Leonhardt, P.Moll, T.Pompl, H.Reisinger, S. Rongen, A. Saenger, U. Schroeder, B. Sell, A. Wahl and D. Schumann, *Tech. Digest IEDM* **2001**, *18.6* (7) J. Klootwijk, A. Kemmeren, R. Wolters, F. Roozeboom, J. Verhoeven, E. van den Heuvel, in *'Defects in Advanced High-κ Dielectric Nano-Electronic Semiconductor Devices'*, (E. Gusev, ed.); Springer: Dordrecht, **2006**, p. 17. (8) S.B.S. Heil, E. Langereis, F. Roozeboom, M.C.M. van de Sanden and W.M.M. Kessels, J. *Electrochem. Soc.* **2006**, 153, G956-G965.

Additional Volatile Precursors for Chemical Vapor and Atomic Layer Deposition

Metal	Volatile Precursor	Linear Formula	Physical State/ Handling Precautions	Purity %	Product No.
Aluminum	Diethylaluminum ethoxide	$(C_2H_5)_2AlOC_2H_5$	Liquid, pyrophoric	97	**256749-100G**
	Trimethylaluminum [TMA]	$Al(CH_3)_3$	Liquid, pyrophoric	97	**257222-100G**
	Tris(dimethylamido)aluminum(III)	$Al(N(CH_3)_2)_3$	Solid, air/moisture -sensitive	>98	**469947-10G**
Hafnium	Tetrakis(diethylamidohafnium(IV) [TDEAT]	$Hf[N(CH_2CH_3)_2]_4$	Liquid, air/moisture -sensitive	99.99	**455202-10G** **455202-25G** **455202-100G**
	Tetrakis(dimethylamido)hafnium(IV) [TDMAH]	$Hf[N(CH_3)_2]_4$	Solid, air/moisture -sensitive	99.99	**455199-5G** **455199-25G**
	Tetrakis(ethylmethylamido)hafnium(IV)	$Hf[N(CH_3)C_2H_5)]_4$	Liquid, air/moisture -sensitive	99.99	**553123-5ML** **553123-25ML**
Tantalum	Tris(diethylamido)(ethylimido)tantalm(V)	$C_2H_5N=Ta(N(C_2H_5)_2)_3$	Liquid, air/moisture -sensitive	99.99	**517836-5ML**
	Tris(diethylamido)(*tert*-butylimido)-tantalum(V)	$(CH_3)_3CN=Ta(N(C_2H_5)_2)_3$	Liquid, air/moisture -sensitive	99.99	**521280-5ML**
	Tris(ethylmethylamido) (*tert*-butylimido)tantalum(V)	$(CH_3)_3CN=Ta(N(C_2H_5)CH_3)_3$	Liquid, air/moisture -sensitive	99.99	**J100043-5G**
Titanium	Bis(diethylamido)bis-(dimethylamido)titanium(IV)	$Ti(N(CH_3)_2)_2(N(CH_2CH_3)_2)_2$	Liquid, air/moisture -sensitive	99.99	**J100026-10G**
	Titanium(IV) chloride [TICL]	$TiCl_4$	Liquid, air/moisture -sensitive	99.995	**254312-10G** **254312-25G**
	Tetrakis(diethylamido)titanium(IV) [TDEAT]	$Ti[N(C_2H_5)_2]_4$	Liquid, air/moisture -sensitive	99.999	**469866-5G** **469866-25G**
	Tetrakis(dimethylamido)titanium(IV) [TDMAT]	$Ti[N(CH_3)_2]_4$	Liquid, air/moisture -sensitive	99.999	**469858-5G** **469858-25G**
	Tetrakis(ethylmethylamido)titanium(IV) [TEMAT]	$Ti(N(C_2H_5)CH_3)_4$	Liquid, air/moisture -sensitive	99.99	**473537-5G** **473537-25G**

For a complete list of metal precursors for CVD/ALD, visit sigma-aldrich.com/precursors.

TO ORDER: Contact your local Sigma-Aldrich office (see back cover), call 1-800-325-3010 (USA), or visit sigma-aldrich.com/matsci.

Vacuum Deposited Non-Precious Metal Catalysts for PEM Fuel Cells

Dr. David G. O'Neill, Dr. Radoslav Atanasoski (pictured) Alison K. Schmoeckel, Alison K. Schmoeckel, George D. Vernstrom, Dennis P. O'Brien, Dr. Manish Jain, Dr. Thomas E. Wood, The 3M Company

Current PEM fuel cell technology uses platinum as a catalyst. A large body of work seeking to find a Pt replacement involves Oxygen Reduction Reaction (ORR) catalysts produced using nitrogen coordinated transition metal compounds, such as Fe porphyrins or Fe phthalocyanine.[1,2,3] Traditionally, these catalysts are made by pyrolyzing transition metal compounds dried onto carbon support particles at temperatures up to 950 °C in reducing and/or nitrogen-containing atmosphere. Unfortunately, ORR activity of these catalysts has not been enough and attempts to increase the oxygen activity, for example by increasing the Fe content, have not been successful.[4] Analytical work by Dodelet's group, including TOF-SIMS, XPS and other techniques, led to their proposal that a pyridinic structure is required for good oxygen activity.[5,6]

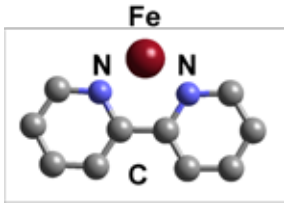

Figure 1. Structure proposed by Dodelet's group[6] for the species required for ORR catalytic activity.

A new, alternative process to make non-precious ORR metal catalysts for the oxygen reduction reaction is to use vacuum deposition techniques to combine the three elements believed to be required (a transition metal, carbon, and nitrogen).[7,8] Processes including pulsed arc plasma deposition, sputter deposition, evaporation and combinations thereof have been used to produce a variety of materials whose catalytic activity was determined by assembling and measuring the oxygen generated electrical current in 50 cm^2 fuel cells. The pulsed arc process is well suited to deposit carbon/Fe based catalysts because it can produce a carbon/iron plasma by erosion of a high-purity graphite cathode containing Fe wires.[9] The plan is to vary deposition processes and conditions over a wide range while checking their catalytic activity in a 50 cm^2 test fuel cell fixture.[10,11] However, solely relying on fuel cell testing does not provide clues to process changes that would be most beneficial, but an analytical technique has not been identified that uniquely qualifies catalytic behavior. Nevertheless, an ability to measure a material characteristic that is known to relate to ORR catalysis would significantly improve process R&D.

Therefore, we began using local, element-specific, analytical probes that have the ability to differentiate between Fe-based catalyst materials that have had different process histories but similar compositions. Vacuum deposited C-Nx:Fe catalysts were analyzed using Extended X-ray Absoption Fine Structure (EXAFS) analyses of the Fe k-edge and resonant ultraviolet photoelectron spectroscopy (UPS) to measure the valence electronic structure around Fe atoms. Both techniques show significant differences between samples that received and those that did not, receive thermal treatment.

Results

Carbon-nitrogen-iron coatings were deposited onto either a carbon non-woven cloth or Si wafers, depending on the analytical technique to be used, and processed either with or without a thermal treatment. Surface composition measurements by XPS showed that the nitrogen and iron content could be varied between 1–5 at. % for nitrogen and between 0.1 to 7 at. % for iron. This range is much larger than can be obtained with molecular pyrolysis methods (2–3 at. % nitrogen and 0.05 at. % Fe). Analysis of the Fe core level indicates that the iron in these coatings is neither metallic nor an oxide; however some carbide phase cannot be ruled out. High resolution XPS shows that the N 1S core level in vapor deposited C-N_x:Fe coatings has the same doublet structure with a component at 398.5 eV, identified as pyridinic nitrogen, that has been reported for pyrolyzed Fe-derived catalyst materials.[6] The fact that the nitrogen exhibits the same XPS fingerprint as pyrolyzed Fe catalysts combined with the fact that the nitrogen and iron content is much higher than in pyrolyzed Fe catalysts suggested that the catalytic currents would be higher. However, our electrochemical fuel cell testing showed the opposite to be true. Although a direct comparison is difficult, after correcting for large differences in surface area, the ORR catalytic activity of vapor deposited coatings is lower than that of pyrolyzed Fe catalysts. Although a thermal treatment above 650 °C, either during or after deposition, significantly increased catalytic activity the level was still below that of pyrolyzed molecular compounds.

The similarity of vacuum deposited coatings based on XPS spectra and the difference in their electrochemical behavior suggests that more detailed materials characterization is needed. Detailed analyses of the N 1S core-level shows that the intensity and binding energy of the 398.5 eV component, the component normally associated with pyridinic nitrogen, changes with iron content. For example, in C-N_x:Fe(7 at. %) the intensity is 75% of the total N 1S intensity, whereas in a nitrogenated carbon (i.e. without iron) the intensity is only 45% of the total. Indeed, the pyridinic component intensity steadily increases as the Fe content increases, as shown by the graph in **Figure 2**. In addition, the pyridinic components binding energy increases with increasing iron content. The shift to deeper binding energy is similar to findings by Dodelet's group for pyrolyzed Fe-derived catalysts, although in those materials the shift is much less.[6] The fact that a small amount of iron has such an effect on the nitrogen core level binding energy suggests that Fe and N atoms are near each other instead of being uniformly dispersed.

Vacuum Deposited Non-Precious Metal Catalysts
Order: 1.800.325.3010 Technical Service: 1.800.231.8327
ALDRICH®

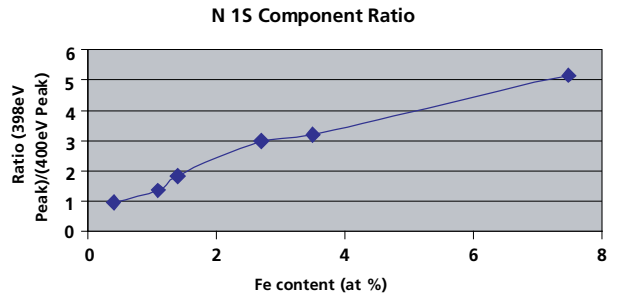

Figure 2. Relative intensity of the N 1S peak at 398.5 eV associated with pyridinic nitrogen as a function of Fe content.

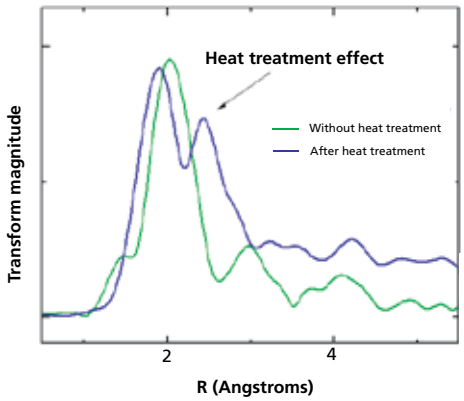

Figure 3. The k^3-weighted Fourier transform magnitudes of the Fe K-edge of a vacuum deposited catalyst before and after the thermal post-treatment. The transforms are not phase-corrected.

Figure 3 shows EXAFS Fourier transforms for vacuum deposited catalysts. These transforms are not phase-corrected and therefore they have a small shift in the x-axis from real values. Examination of Figure 3 shows that the unheated material has a single main peak while the heated sample has two well-resolved peaks. This indicates that the as-deposited material is fairly disordered and that heating increases atomic order (narrower peaks) with the introduction of a second coordination shell around Fe atoms. Photoelectron spectroscopy is another technique that has the potential to identify unique aspects of C-N_x:Fe materials because it directly probes valence electrons that are involved in bonding, and many believe catalysis. Photoemission is not, in general, element specific, however, element specific information can be obtained by utilizing resonant photoemission. In resonant photoemission, large intensity variations occur with small changes in the exciting photon energy and this can be used to detect where Fe d-states are located in the valence density-of-states.[12] The role of Fe and it's importance for catalytic behavior, many believe, is key to understanding Fe-based catalysts. We have successfully used photoemission to study C-N_x:Fe materials including the use of resonant techniques to detect valence Fe d-states. These studies, to be published, show that metallic Fe d-states exist near the Fermi level in as-deposited coatings as well as hybridized d-states between 4 to 10 eV below the Fermi level. Photoemission studies combined with *ab initio* density functional theory simulations, using VASP,[12,13] has the potential to provide new insights into bonding in ORR Fe-based catalysts.

Conclusions

Vacuum deposited carbon-nitrogen-iron coatings deposited by pulsed cathodic arc plasma deposition were characterized and the effects of a high temperature thermal treatment were evaluated. Characterization by XPS shows that the iron is not metallic iron and that the N 1S core level matches that found in pyrolyzed Fe-based catalysts. High resolution XPS studies of the N 1S core level vs. Fe content shows that Fe atoms cause the N 1S core level component at about 398.5 eV, also associated with pyridinic nitrogen, to increase in intensity and to shift to deeper binding energy. Clearly, Fe atoms must be near nitrogen atoms in order to change N 1S binding energies.

Subjecting the vapor deposited catalysts to a thermal treatment, either during or after deposition, significantly increases the catalytic activity of these materials. However, comparison of these materials, with and without a thermal treatment, using high resolution XPS does not show significant differences. EXAFS studies of the Fe k-edge show that atomic rearrangements occur after high temperature treatments, thermal treatments that also increase ORR catalytic currents. The thermal treatment increases atomic order and introduces a second coordination shell around Fe atoms. Resonant UV photoemission techniques show that Fe d-electrons are located in two energy regions of the electronic density of states. There are metallic Fe d-states located near the Fermi level and hybridized Fe d-states, most likely with ligand p-states, located between 4 to 12 eV below the Fermi level. More work is needed with different materials before more conclusive statements can be made.

Element specific techniques such as EXAFS and resonant photoemission show promise in being able to detect changes around given atoms, e.g. iron, in a ternary compound such as the C-N_x:Fe materials that exhibit catalytic activity for the oxygen-reduction reaction. Changes that are associated with better catalytic activity. Although the vapor deposited materials made so far have not exhibited significant ORR catalytic activity, future developments and improved understanding of these materials could allow vapor deposition to be a viable process for economical catalyst production.

Acknowledgments

This research was supported in part by the Department of Energy, Cooperative Agreement No. DE-FC36-03GO13106. DOE support does not constitute an endorsement by DOE of the views expressed in this article. The authors would like to thank our colleagues at 3M, particularly Dr. Shih-Hung Chou, Dr. Allen Siedle, and Terry Pechacek; Drs. Xiao-Qing Yang and Won-Sub Soon at Brookhaven National Laboratory; Dr. Cliff Olson at the Synchrotron Radiation Center; and Professor David Wieliczka at University of Missouri - KC. The authors would also like to thank Professor Jeff Dahn and his research group, Dalhousie University, for useful conversations, and Professor Jean-Pol Dodelet and his group, INRS-Energie, Materiaux et Telcommunications, for the samples provided for this study.

TO ORDER: Contact your local Sigma-Aldrich office (see back cover),
call 1-800-325-3010 (USA), or visit sigma-aldrich.com/matsci.

References and Note
(1) Terminology Convention: "pyrolyzed, Fe-derived" will refer to the catalyst syntheses using Fe containing molecules, such as Fe porphoryns, Fe phthalocyanines, Fe-acetate, etc. (2) N4-Macrocyclic Metal Complexes: Electrocatalysis, Electrophotochemistry & Biomimetic Electroanalysis. Edited by J. Zagal, F. Bedioui, and J. P. Dodelet, Springer **2006**. (3) H. A. Gasteiger, S. S. Kocha, B. Sompalli, F. T. Wagner, *Applied Cat. B: Environ.*, **2005**, *9,* 56. (4) J.-P. Dodelet in N4-Macrocyclic Metal Complexes: Electrocatalysis, Electrophotochemistry & Biomimetic Electroanalysis. Edited by J. Zagal, F. Bedioui, and J. P. Dodelet, Springer **2006**. (5) F. Jaouen, M. Lefevre, J.-P. Dodelet, and M. Cai, *J. Phys. Chem. B*, **2006**, *5553*, 110. (6) F. Jaouen, S. Marcott, J.-P. Dodelet and G. Lindbergh, *J. Phys. Chem. B,* **2003**, *1376,* 107. (7) R.T. Atanasoski, *Novel Approach to Non-Precious Metal Catalysts*, DOE Hydrogen Program FY **2004** Progress Report (V.C.5). (8) G. Lalande, D. Guay, J. P. Dodelet, S. A. Majetich, M.E.McHenry, *Chem. Mater.*, **1997**, *784,* 9. E. Bradley Easton, Arman Bonakdarpour, and J.R. Dahn, *Electrochem. and Solid-State Lett.*, **2006**, *A463,* 9. (9) E.I. Tochitsky, O.V. Selifanov, V.V. Akulich, I.A. Kapustin and A.V. Stanishevskii, *Surface and Coatings Technology*, 1991 522, 47. (10) R.T. Atanasoski, *Novel Approach to Non-Precious Metal Catalysts*, DOE Hydrogen Program FY **2005** Progress Report (V.C.5). (11) R.T. Atanasoski, *Novel Approach to Non-Precious Metal Catalysts*, DOE Hydrogen Program FY **2006** Progress Report. (12) G. Kresse and J. Hafner, *Phys. Rev. B*, **47**, 558 (1993); G. Kresse and J. Furthmüller, *Phys. Rev. B*, **1996**, *11169,* 54. G. Kresse and J. Furthmüller, *Comput. Mater. Sci.*, **1996**, *15,* 6. G. Kresse and D. Joubert, *Phys. Rev. B*, **1999**, *1758,* 59. (13) M. Jain, S.-H. Chou, A. Siedle, *J. Phys. Chem. B*, **2006**, *4179,* 110.

High-Purity Graphite and Iron

Materials	Physical Form	Size/density	Purity (%)	Product No.
Iron	Wire	diam. 0.5 mm	99.99	**266248-7.5G**
		diam. 1.0 mm	99.99	**266256-3.1G** **266256-15.5G**
		diam. 0.5 mm	99.9	**356832-1.5G** **356832-7.5G**
		diam. 1.0 mm	99.9	**356824-6.2G** **356824-31G**
	Foil	thickness 0.25 mm	99.99	**338141-1.2G** **338141-5G**
		thickness 0.1 mm	99.9	**356808-2G** **356808-8G**
	Granule	10–40 mesh	99.999	**413054-5G** **413054-25G**
	Rod	diam. 6.3 mm	99.98	**266213-30G** **266213-150G**
Graphite	Rod	length 150 mm, diam. 3 mm, low density	99.999	**496537-43.5G**
		length 150 mm, diam. 3 mm, high density	99.995	**496545-60G**
		length 150 mm, diam. 6 mm, low density	99.999	**496553-180.7G**
		length 150 mm, diam. 6 mm, high density	99.995	**496561-240.5G**

SIGMA-ALDRICH LECTURE-BOTTLE STATIONS

Safe and Simple Systems for Dispensing Lecture-Bottle Gases

Dispensing lecture-bottle gases has never been safer or simpler using these portable lecture-bottle stations. The premium quality components housed within a station are matched to the application, fully assembled, leak-tested, and ready for use. Just connect the station to the lecture-bottle, process, and a source of inert gas if using a station with a purge valve, and you are ready to go.

Safe and Simple

- Gas dispensing and storage in one compact, portable system
- Keeps lecture-bottles upright and stable, eliminates tip-over
- Reduces equipment damage and chance of personal injury
- Choice of four models matched to the application
- Wall-mountable
- Express Service™ Program for fast cleaning, repair, or component replacement

Order Information

Description	Prod. No.
Non-Corrosive Lecture-Bottle Station	**Z562599**-1EA
High-Purity Lecture-Bottle Station	**Z562602**-1EA
Lecture-Bottle Station with T-Purge Valve	**Z562610**-1EA
Corrosive Lecture-Bottle Station with Cross-Purge Valve	**Z562629**-1EA
Lecture-Bottle Service Station	**Z562637**-1EA

Visit our Web site for a brochure with complete information about these new Lecture-Bottle dispensing stations, including a Station Selection Guide that matches the correct station to the gas you are using.

sigma-aldrich.com/gases

For questions, product data, or new product suggestions, please contact the Materials Science team at matsci@sial.com.

Order: 1.800.325.3010 Technical Service: 1.800.231.8327

Argentina
SIGMA-ALDRICH DE ARGENTINA, S.A.
Tel: 54 11 4556 1472
Fax: 54 11 4552 1698

Australia
SIGMA-ALDRICH PTY., LIMITED
Free Tel: 1800 800 097
Free Fax: 1800 800 096
Tel: 612 9841 0555
Fax: 612 9841 0500

Austria
SIGMA-ALDRICH HANDELS GmbH
Tel: 43 1 605 81 10
Fax: 43 1 605 81 20

Belgium
SIGMA-ALDRICH NV/SA.
Free Tel: 0800-14747
Free Fax: 0800-14745
Tel: 03 899 13 01
Fax: 03 899 13 11

Brazil
SIGMA-ALDRICH BRASIL LTDA.
Tel: 55 11 3732-3100
Fax: 55 11 3733-5151

Canada
SIGMA-ALDRICH CANADA LTD.
Free Tel: 800-565-1400
Free Fax: 800-265-3858
Tel: 905-829-9500
Fax: 905-829-9292

China
SIGMA-ALDRICH (SHANGHAI)
TRADING CO. LTD.
Tel: +86-21-61415566
Fax: +86-21-61415567

Czech Republic
SIGMA-ALDRICH S.R.O.
Tel: +420 246 003 200
Fax: +420 246 003 291

Denmark
SIGMA-ALDRICH DENMARK A/S
Tel: 43 56 59 10
Fax: 43 56 59 05

Finland
SIGMA-ALDRICH FINLAND
Tel: (09) 350 9250
Fax: (09) 350 92555

France
SIGMA-ALDRICH CHIMIE S.à.r.l.
Tel appel gratuit: 0800 211 408
Fax appel gratuit: 0800 031 052

Germany
SIGMA-ALDRICH CHEMIE GmbH
Free Tel: 0800-51 55 000
Free Fax: 0800-649 00 00

Greece
SIGMA-ALDRICH (O.M.) LTD
Tel: 30 210 9948010
Fax: 30 210 9943831

Hungary
SIGMA-ALDRICH Kft
Tel: 06-1-235-9054
Fax: 06-1-269-6470
Ingyenes zöld telefon: 06-80-355-355
Ingyenes zöld fax: 06-80-344-344

India
SIGMA-ALDRICH CHEMICALS
PRIVATE LIMITED
Telephone
Bangalore: 91-80-6621-9600
New Delhi: 91-11-4165-4255
Mumbai: 91-22-2570-2364
Hyderabad: 91-40-6684-5488
Fax
Bangalore: 91-80-6621-9650
New Delhi: 91-11-4165-4266
Mumbai: 91-22-2579-7589
Hyderabad: 91-40-6684-5466

Ireland
SIGMA-ALDRICH IRELAND LTD.
Free Tel: 1800 200 888
Free Fax: 1800 600 222
Tel: 353 1 4041900
Fax: 353 1 4041910

Israel
SIGMA-ALDRICH ISRAEL LTD.
Free Tel: 1-800-70-2222
Tel: 08-948-4100
Fax: 08-948-4200

Italy
SIGMA-ALDRICH S.r.l.
Telefono: 02 33417310
Fax: 02 38010737
Numero Verde: 800-827018

Japan
SIGMA-ALDRICH JAPAN K.K.
Tokyo Tel: 03 5796 7300
Tokyo Fax: 03 5796 7315

Korea
SIGMA-ALDRICH KOREA
Tel: 031-329-9000
Fax: 031-329-9090

Malaysia
SIGMA-ALDRICH (M) SDN. BHD
Tel: 603-56353321
Fax: 603-56354116

Mexico
SIGMA-ALDRICH QUÍMICA, S.A. de C.V.
Free Tel: 01-800-007-5300
Free Fax: 01-800-712-9920

The Netherlands
SIGMA-ALDRICH CHEMIE BV
Tel Gratis: 0800-0229088
Fax Gratis: 0800-0229089
Tel: 078-6205411
Fax: 078-6205421

New Zealand
SIGMA-ALDRICH PTY., LIMITED
Free Tel: 0800 936 666
Free Fax: 0800 937 777
Tel: 61 2 9841 0500
Fax: 61 2 9841 0500

Norway
SIGMA-ALDRICH NORWAY AS
Tel: 23 17 60 60
Fax: 23 17 60 50

Poland
SIGMA-ALDRICH Sp. z o.o.
Tel: 061 829 01 00
Fax: 061 829 01 20

Portugal
SIGMA-ALDRICH QUÍMICA, S.A.
Free Tel: 800 202180
Free Fax: 800 202178
Tel: 21 9242555
Fax: 21 9242610

Russia
SIGMA-ALDRICH RUS, LLC
Tel: +7 (495) 621-5828/5923/6037
Fax: +7 (495) 621-5828/5923/6037

Singapore
SIGMA-ALDRICH PTE. LTD.
Tel: 65-67791200
Fax: 65-67791822

South Africa
SIGMA-ALDRICH
SOUTH AFRICA (PTY) LTD.
Free Tel: 0800 1100 75
Free Fax: 0800 1100 79
Tel: 27 11 979 1188
Fax: 27 11 979 1119

Spain
SIGMA-ALDRICH QUÍMICA, S.A.
Free Tel: 900 101376
Free Fax: 900 102028
Tel: 91 661 99 77
Fax: 91 661 96 42

Sweden
SIGMA-ALDRICH SWEDEN AB
Tel: 020-350510
Fax: 020-352522
Outside Sweden Tel: +46 8 7424200
Outside Sweden Fax: +46 8 7424243

Switzerland
SIGMA-ALDRICH CHEMIE GmbH
Swiss Free Call: 0800 80 00 80
Tel: +41 81 755 2828
Fax: +41 81 755 2815

United Kingdom
SIGMA-ALDRICH COMPANY LTD.
Free Tel: 0800 717181
Free Fax: 0800 378785
Tel: 01747 833000
Fax: 01747 833313
SAFC (UK): 01202 712305

United States
SIGMA-ALDRICH
P.O. Box 14508
St. Louis, Missouri 63178
Toll-Free: (800) 325-3010
Call Collect: (314) 771-5750
Toll-Free Fax: (800) 325-5052
Tel: (314) 771-5765
Fax: (314) 771-5757

Internet
sigma-aldrich.com

World Headquarters
3050 Spruce St., St. Louis, MO 63103
(314) 771-5765
sigma-aldrich.com

Order/Customer Service (800) 325-3010 • Fax (800) 325-5052
Technical Service (800) 325-5832 • sigma-aldrich.com/techservice
Development/Bulk Manufacturing Inquiries SAFC™ (800) 244-1173

SIGMA-ALDRICH

*Accelerating Customers' Success through Leadership in **Life Science**, **High Technology** and **Service***

The SIGMA-ALDRICH Group

SIGMA® ALDRICH® Fluka® Riedel-de Haën® SAFC® SUPELCO® ISOTEC™

©2006 Sigma-Aldrich Co. All rights reserved.
SIGMA, SAFC, SAFC™, SIGMA-ALDRICH, ISOTEC, ALDRICH, FLUKA, and SUPELCO are trademarks belonging to Sigma-Aldrich Co. and its affiliate Sigma-Aldrich Biotechnology, L.P. Riedel-de Haën® trademark under license from Riedel-de Haën GmbH. Sigma brand products are sold through Sigma-Aldrich, Inc.
Sigma-Aldrich, Inc. warrants that its products conform to the information contained in this and other Sigma-Aldrich publications. Purchaser must determine the suitability of the product(s) for their particular use. Additional terms and conditions may apply. Please see reverse side of the invoice or packing slip.

JCU
01671-503403
0116

SIGMA-ALDRICH

3050 Spruce Street • St. Louis, MO 63103 USA

Return Service Requested

PRESORTED
STANDARD
U.S. POSTAGE
PAID
SIGMA-ALDRICH
CORPORATION